Int J Biometeorol (2012) 56:411–418
DOI 10.1007/s00484-011-0445-2

SHORT COMMUNICATION

Testing the hypothesis on the relationship between aerodynamic roughness length and albedo using vegetation structure parameters

Jaeil Cho · Shin Miyazaki · Pat J.-F. Yeh · Wonsik Kim · Shinjiro Kanae · Taikan Oki

Received: 17 January 2011 / Revised: 20 April 2011 / Accepted: 21 April 2011 / Published online: 12 May 2011

Abstract Surface albedo (α) and aerodynamic roughness length (z_0), which partition surface net radiation into energy fluxes, are critical land surface properties for biosphere–atmosphere interactions and climate variability. Previous studies suggested that canopy structure parameters influence both α and z_0; however, no field data have been reported to quantify their relationships. Here, we hypothesize that a functional relationship between α and z_0 exists for a vegetated surface, since both land surface parameters can be conceptually related to the characteristics of canopy structure. We test this hypothesis by using the observed data collected from 50 site-years of field measurements from sites worldwide covering various vegetated surfaces. On the basis of these data, a negative linear relationship between α and $\log(z_0)$ was found, which is related to the canopy structural parameter. We believe that our finding is a big step toward the estimation of z_0 with high accuracy. This can be used, for example, in the parameterization of land properties and the observation of z_0 using satellite remote sensing.

Keywords Albedo · Roughness length · Canopy structural parameter

J. Cho (✉)
Kasuya Research Forest, Kyushu University,
Sasaguri, Fukuoka 811–2415, Japan
e-mail: chojaeil@gmail.com

S. Miyazaki
Graduate School of Environmental Science, Hokkaido University,
N10W5,
Sapporo 060–0810, Japan

P. J.-F. Yeh · T. Oki
Institute of Industrial Science, The University of Tokyo,
4-6-1 Komaba,
Meguro-ku, Tokyo 153–8505, Japan

W. Kim
National Institute for Agro-Environmental Sciences,
3-1-3 Kannondai,
Tsukuba, Ibaraki 305–8604, Japan

S. Kanae
Department of Mechanical and Environmental Informatics, Tokyo Institute of Technology,
2-12-1 O-okayama,
Meguro-ku, Tokyo 152–8552, Japan

Introduction

Considerable evidence supports the idea that the interactions between the land surface and the atmosphere modulate surface energy partitioning and water balance, and consequently impact climate variability (Sellers et al. 1997). The conditions of the terrestrial ecosystems typically exert great influence on regional climate and global circulation (Betts et al. 1997). Among land surface properties, albedo and roughness length (z_0) are two of the most critical parameters for the partitioning of available surface energy into latent, sensible, and ground heat fluxes in the land surface–atmosphere interactions (Garratt 1994; Bonan 2002).

Land surface albedo (α), the proportion of solar radiation reflectance from the surface, determines the energy available for physical and biochemical processes, whereas the aerodynamic roughness length (z_0), an index of aerodynamic turbulence, is associated with the exchange of momentum, energy, and trace gases between the biosphere and atmosphere. The alteration in α and z_0 induced by land cover change significantly affects local and regional climates. Previous climate model studies on the impacts of deforestation have indicated that these properties are the key functional land factors that affect the boundary conditions

in global climate simulations (Lean and Warrilow 1989; Hahmann and Dickinson 1997; Henderson-Sellers et al. 1993). For example, the replacement of the dominant α and z_0 values of forest with those of bare ground in deforestation experiments leads to a decrease in both evaporation and precipitation on a regional scale. Such types of macroclimate change will also potentially lead to further regional vegetation change as an atmosphere–biosphere feedback (Kanae et al. 2001).

The specification of α and z_0 parameters in climate models is traditionally based on the prescribed look-up tables according to a rough classification of dominant vegetation types (Henderson-Sellers et al. 1993; Kanae et al. 2001). Although α and z_0 are calculated in certain more advanced climate models, such estimation is still strongly dependent on the optical properties of the single-leaf and canopy height parameters, which traditionally are also determined from the look-up table of vegetation types (Betts et al. 1997). This approach may not be sufficiently precise for the climate modeling application considering the large spatial heterogeneity involved at the global scale and the dynamic vegetation transition from the interannual to decadal timescales.

In this study, we hypothesize that, although there is no direct causation between α and z_0, a functional relationship between them can be sought for a vegetated surface, since both land surface parameters are conceptually related to vegetation structure parameters [e.g., leaf area index (LAI), canopy height (H), canopy density, crown area, etc.]. We test this hypothesis by using the observed data of α, z_0, and vegetation structure parameters collected from 50 site-years of field measurements from sites worldwide covering various vegetated surfaces. Our expectation is that, if an explicit functional relationship among α, z_0, and vegetation structure parameters, can be identified, it would significantly enhance the scientific understanding of the formation of vegetation functional and structural parameters and would also improve the parameterization of surface energy and water balances in climate modelling.

Data

α and z_0 in individual places are commonly evaluated from the tower-based flux measurement sites, which are the exchanges of energy and the biogeochemical dynamic of traces gases between the atmosphere and the plant ecosystems. Major vegetation structural parameters, LAI and H, are considered as information about land surface characteristics in most sites (Baldocchi et al. 2001). By searching the literature as well as through personal communications with individual data owners, we have collected and compiled data on the vegetation functional and structure parameters at 50 site-years of field measurements (Table 1).

The parameters α and z_0 (particularly the latter) are in general difficult to measure. α is commonly measured using downward- and upward-facing radiometers installed on the measurement towers. z_0 is traditionally referred to in the context of the Monin–Obukhov similarity law using the wind speed profile (Brutsaert 1982; Oke 1987). However, due to its measurement difficulties, the various semi-empirical or empirical methods of particular surface condition-dependent parameters have been developed (Martano 2000). In this study, the values of α and z_0 reported from each measurement site and their published literature are used in the following analysis to test our hypothesis. The compiled data used in this study (Table 1) include LAI, H, midday α and z_0 covering various vegetation types including forest, grass, crop, shrub and semi-desert. The data were measured at the peak of the leaf biomass in the specified year for each site and categorized by the international geosphere–biosphere program (IGBP) vegetation classification system.

Statement of hypothesis

In general, the presence of vegetation decreases α and increases z_0 (Monteith and Unsworth 2008) because the vegetation conditions will mainly control the variations of α and z_0. Li et al. (2000) and Thompson et al. (2004) empirically represented the relationship between α and the total biomass. The horizontal and vertical distribution of vegetation has a dominant effect on the radiation penetration and backscatter, as well as on the wind drag. In fact, besides canopy structure from biomass, the dependence of α to the amount of plant chlorophyll has also been reported (Ollinger et al. 2008; Hollinger et al. 2010). It implies that the total biomass product forms into vegetation morphological characteristics for photosynthetic elements placed in a functionally optimum position through the allometric scaling law (Enquist et al. 1998; Price et al. 2007). Eventually, these show that canopy structure can be considered as the common causative factor in the formation of α and z_0 on the vegetated surface (Nakai et al. 2008). Accordingly, in this section we will discuss the possible ways of representing functional relationship among α, z_0, and vegetation structure parameters.

A canopy structure is defined as the organization in space and time of the bulk plant components such as foliage/leaves and stems (Parker 1995). The richness and variety of plant types and sizes imply structural complexity of plant organizations (Green et al. 2006), which can be described by the spatial distribution of biomass products (Parker and Russ 2004). In previous studies, several functional parameters were suggested to indicate the vegetation canopy structure. First, the “rugosity” of the outer canopy surface can be measured as the standard

Table 1 The data on the vegetation functional and structure attributes at 50 site-years of field measurements from sites worldwide

No.	Site	Latitude	Longitude	Vegetation type[a]	LAI[b]	H[b]	α[b]	z_0[b]	Reference
1	Niwot Ridge	40°02′N	105°33′W	(F) Evergreen needleleaf	4.0	11.4	0.131	1.620	Turnipseed et al. (2003)[c]
2	Campbell River	49°52′N	125°20′W	(F) Evergreen needleleaf	7.3	33.0	0.093	3.000	Chen et al. (2006)[c]
3	Wind River Crane	45°49′N	121°57′W	(F) Evergreen needleleaf	8.6	60.0	0.071	6.000	Thomas and Winner (2000)[c]
4	Missouri Ozark	38°45′N	92°12′W	(F) Deciduous broadleaf	5.3	18.0	0.120	2.103	Gu et al. (2006)[c]
5	Willow Creek	45°48′N	90°05′W	(F) Deciduous broadleaf	5.3	24.0	0.165	2.300	Cook et al. (2004)[c]
6	Morgan-Monroe	39°19′N	86°25′W	(F) Deciduous broadleaf	4.7	26.0	0.150	2.100	Schmid et al. (2000)[c]
7	Fujiyoshida	35°45′N	138°80′E	(F) Evergreen needleleaf	4.8	19.0	0.093	1.850	Ohtani et al. (2001)[c]
8	Bayreuth	50°09′N	11°52′E	(F) Evergreen needleleaf	5.0	19.0	0.080	2.000	Thomas and Foken (2007)[c]
9	Bankenbosch (SLIMM tower)	53°01′N	06°25′W	(F) Deciduous needleleaf	1.8	19.7	0.100	2.100	Klaassen et al. (2002)[c]
10	Hainich	51°05′N	10°27′E	(F) Deciduous broadleaf	5.0	33.0	0.160	2.500	Knohl et al. (2003); during summer
11	Bordeaux	44°42′N	00°46′W	(F) Evergreen needleleaf	5.5	18.0	0.104	1.900	Berbigier et al. (2001)[c]
12	Norunda	60°05′N	17°28′E	(F) Evergreen needleleaf	4.8	25.0	0.084	1.750	Mölder and Lindroth (1999)[c]
13	Loobos	52°10′N	05°45′E	(F) Evergreen needleleaf	1.9	16.6	0.090	1.500	Dolman et al. (2002)[c]
14	Hyytiala	61°51′N	24°17′E	(F) Evergreen needleleaf	3.0	14.0	0.125	1.000	Suni et al. (2003)[c]
15	Tharandt	50°58′N	13°34′E	(F) Evergreen needleleaf	7.6	26.5	0.076	2.250	Grünwald and Bernhofer (2007)[c]
16	Petsikko	69°28′N	27°14′E	(F) Deciduous broadleaf	2.5	3.5	0.159	0.500	Laurila et al. (2001); during summer
17	Council forest	64°54′N	163°40′W	(F) Evergreen needleleaf	2.8	6.1	0.100	1.600	Beringer et al. (2005); Thompson et al. (2004)
18	Landes forest	.	.	(F) Evergreen needleleaf	.	.	0.100	2.350	Mahrt and Ek (1993)[d]
19	Southern BOREAS area	.	.	(F) Evergreen needleleaf	.	.	0.095	1.560	Betts et al. (2007)[d]; Black spruce site
20	Southern BOREAS area	.	.	(F) Evergreen needleleaf	.	.	0.100	1.730	Betts et al. (2007)[d]; Forest site
21	Ibaraki	34°55′N	135°45′E	(F) Evergreen needleleaf	.	.	0.110	0.700	Hattori et al. (1993)
22	Reserva Florestal Ducke	02°57′S	59°57′W	(F) Evergreen broadleaf	.	.	0.120	2.200	Shuttleworth et al. (1989)
23	Coniferous forest site (9a)[e]	.	.	(F) Evergreen needleleaf	3.1	22.0	0.095	0.660	Jarvis et al. (1976)[f]
24	Coniferous forest site (3b)[e]	.	.	(F) Evergreen needleleaf	2.6	14.0	0.150	0.280	Jarvis et al. (1976)[f]
25	Coniferous forest site (17)[e]	.	.	(F) Evergreen needleleaf	4.3	15.5	0.090	0.930	Jarvis et al. (1976)[f]
26	Coniferous forest site (13)[e]	.	.	(F) Evergreen needleleaf	8.4	27.2	0.040	5.032	Jarvis et al. (1976)[f]
27	Coniferous forest site (19)[e]	.	.	(F) Evergreen needleleaf	9.6	11.5	0.150	0.345	Jarvis et al. (1976)[f]
28	Council woodland	64°54′N	163°40′W	(F) Deciduous broadleaf; treeline	2.3	5.10	0.130	0.740	Beringer et al. (2005); Thompson et al. (2004)
29	Wagga	35°04′S	147°20′E	(G) Pasture	0.2	0.20	0.185	0.026	Leuning et al. (2004); during 1994
30	Wagga	35°04′S	147°20′E	(G) Pasture	2.0	0.50	0.181	0.065	Leuning et al. (2004); during 1995
31	Bullenbung	35°07′S	147°02′E	(G) Pasture	0.2	0.10	0.209	0.013	Leuning et al. (2004); during 1994
32	Browning	35°10′S	146°46′E	(G) Pasture	1.5	0.20	0.185	0.026	Leuning et al. (2004); during 1995
33	Urana	35°15′S	146°26′E	(G) Pasture	0.2	0.10	0.230	0.013	Leuning et al. (2004); during 1994
34	Urana	35°16′S	146°24′E	(G) Pasture	1.0	0.20	0.207	0.026	Leuning et al. (2004); during 1995
35	Smileyburg	37°31′N	96°51′W	(G) Tallgrass prairie	2.5	0.15	0.177	0.015	Coulter et al. (2006)
36	Daliushu Village	42°58′N	120°43′W	(G) Sandy grassland	.	.	0.180	0.043	Li et al. (2000)[g]
37	Daliushu Village	42°58′N	120°43′W	(G) Sandy grassland	.	.	0.190	0.129	Li et al. (2000)[g]
38	Daliushu Village	42°58′N	120°43′W	(G) Sandy grassland	.	.	0.180	0.016	Li et al. (2000)[g]
39	Daliushu Village	42°58′N	120°43′W	(G) Sandy grassland	.	.	0.200	0.268	Li et al. (2000)[g]
40	Daliushu Village	42°58′N	120°43′W	(G) Sandy grassland	.	.	0.220	0.004	Li et al. (2000)[g]
41	Daliushu Village	42°58′N	120°43′W	(G) Sandy grassland	.	.	0.200	0.023	Li et al. (2000)[g]
42	Daliushu Village	42°58′N	120°43′W	(G) Sandy grassland	.	.	0.220	0.012	Li et al. (2000)[g]
43	Daliushu Village	42°58′N	120°43′W	(G) Sandy grassland	.	.	0.200	0.009	Li et al. (2000)[g]
44	Daliushu Village	42°58′N	120°43′W	(G) Sandy grassland	.	.	0.200	0.003	Li et al. (2000)[g]
45	De Sinderhoeve	51°35′N	5°27′W	(C) Maize	4.0	2.30	0.200	0.114	Mihailović and Kallos (1997)
46	Southern BOREAS area	.	.	(C) Wheat	.	.	0.100	0.220	Betts et al. (2007)[d]
47	Council Shrubland	64°56′N	164°44′W	(S) Mixed tall shrub	1.9	1.50	0.150	0.180	Beringer et al. (2005); Thompson et al. (2004)

Table 1 (continued)

No.	Site	Latitude	Longitude	Vegetation type[a]	LAI[b]	H[b]	α[b]	z_0[b]	Reference
48	Council low shrubland	64°53′N	163°39′W	(S) Mixed low shrub	1.7	0.25	0.170	0.080	Beringer et al. (2005); Thompson et al. (2004)
49	Heihe River Basin site	.	.	(SD)	.	.	0.210	0.004	Wang et al. (1998); Gobi desert
50	Heihe River Basin site	.	.	(SD)	.	.	0.250	0.005	Wang et al. (1998); sand desert

[a] *F* Forest, *G* grassland, *C* crop, *S* shrub, *SD* semi-desert

[b] *LAI* Leaf area index (m^2 m^{-2}), *H* canopy height (m), α albedo (0–1), z_0 roughness length (m)

[c] Personal communication

[d] Airborne observation data

[e] Site numbers in Jarvis et al. (1976)

[f] Albedo during sunny day,

[g] When vegetation cover fraction is more than 70%

deviation of H. As shown by the Airborne Visible/Infrared Imaging Spectrometer (AVIRIS) data of Ogunjemiyo et al. (2005, see their Fig. 2), rugosity has a strong positive relationship with the shade fraction (sunlit background). Since the shade fraction image can be represented by contrast with the reflectance image, rugosity has been shown to have a negative linear relationship with α (Ogunjemiyo et al. 2005).

Second, the "frontal area index" of roughness elements, which is the horizontally projected area, has been introduced to estimate z_0 (Lettau 1969; Wooding et al. 1973). Although the data of the frontal area index (bH/D^2, where b and D are the averaged breadth and plant density, respectively) is in general not easy to obtain, it is a key parameter to estimate z_0 in the drag partition model (e.g., Raupach 1994; Jasinski et al. 2005). The shade fraction can be related with the frontal area index because both of them provide an efficient measure of plant geometric roughness. Hence, rugosity, which is related to the shade fraction, can have a rather similar meaning to the frontal area index. These inherent relationships between the canopy structural indexes (i.e., rugosity, frontal area index) and α and z_0 will be one part of the evidence to support our hypothesis.

Results and discussion

In Fig. 1, the relationship between α and $\log(z_0)$ are plotted for forest, grass, shrub, crop, and semi-desert on the basis of the data from 50 site-years in Table 1. As shown, vegetated surface has a lower α and a higher z_0 than the semi-desert (mostly bare soil). In addition, forest has a higher z_0 and a lower α than grass because trees have markedly larger plant size and volume protruding from ground than other plant types. Although only a few sites are available in our dataset, the shrub with its plant size between forest and grass has intermediate values of α and z_0. These arguments are consistent with our hypothesis describing the relationship of α and z_0. In Fig. 1, α is generally shown in inverse proportion to z_0, and the relationship between α and $\log(z_0)$ can be fitted by the following linear regression formula:

$$\log(z_0) = -16.80\,\alpha + 1.87 \quad (1)$$

This has a high coefficient of determination R^2=0.76 (P<0.0001), the solid line in Fig. 1. Basically, when the plant size increases, the light resources for plant physiological activities become more limited because of overlapping plant elements (Enquist et al. 1998; Green et al. 2006). For example, canopy structure tends to become more complex through vegetation competition, and the canopy structure

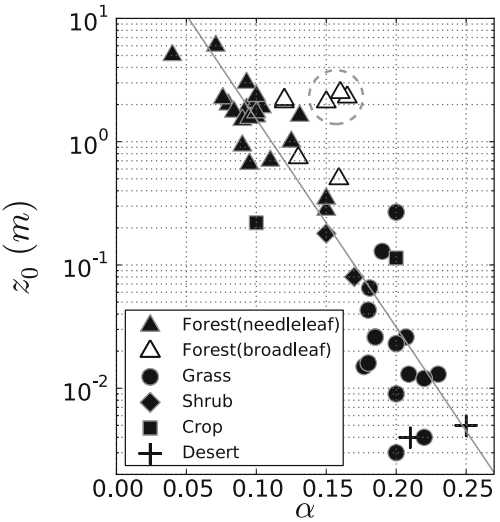

Fig. 1 Scatter plot between α and $\log(z_0)$ for forest (*triangle*), grass (*circle*), shrub (*diamond*), crop (*rectangle*), and semi-desert (*cross*) based on field measurement data (Table 1). *Open-triangle* specifically represents broad-leaf forest. *Gray solid line* is the linear regression between α and $\log(z_0)$ with a R^2=0.76: α is albedo and $\log(z_0)$ is log-scaled roughness length

leads to enhanced penetration of radiation into the canopy and larger aerodynamic drag stress (Eagleson 2002). Hence, the negative relationship between α and z_0 is expressed in order of the vegetation types, which could be listed by the general volume of the total biomass (Fig. 1).

The three open triangles (see the dashed line circle in Fig. 1) representing the group of broad-leaf forest (following the IGBP classification) are the outliers of the regression line (Eq. 1). When assuming the same greenness (plant chlorophyll), the needleleaf and broadleaf forests either will have the same α because of similar optical properties of foliage, or the broadleaf forest has a higher α because solar radiation cannot penetrate deeply because of its broad-faced leaf morphology. Besides, assuming identical biomass and H, the needle-leaf forest tends to have a lower z_0 than the broad-leaf forest primarily because of the vertical accumulation by a single needle-leaf of low aerodynamic drag stress.

In fact, there is slight scattering of individual plots in Fig. 1, in spite of the fact that a remarkably negative linear relationship is found between α and log-scaled z_0. α and z_0 are influenced by not only the vegetation structure but also by many other environmental factors (e.g., the wetted canopy or soil surface). In addition, even though we assumed that the vertical distribution of chlorophyll is related to the formation of canopy structure for optimum physiological function (see Section 3 in Hirose 2005), the difference of a leaf chlorophyll concentration according to plant types (e.g., tropical and temporal broadleaf) or some leaf diseases may be possible to derive deviation in the relationship of α and z_0. In this study, we focus on the "vegetation structure", since it is the common controller for α and z_0 across various vegetation types. Given the diverse surface conditions (e.g., soil, moisture, wind, topography, greenness) among the 50 site-years, a linear relationship between α and z_0 can still be observed, which implies that both α and z_0 are mainly governed by at least one common factor—biomass density, or more generally, vegetation structure.

Conventionally, LAI and H have been utilized as the canopy structural parameter since they represent well the morphological components of vegetation (Brutsaert 1982; Monteith and Unsworth 2008). H indicates the spatial size occupied by plants (Stanhill 1970; Campbell 1973), and LAI represents the amount of photosynthetic elements in plants (Sellers 1985; Choudhury and Monteith 1988). Further, both structural functions significantly influence radiation reflectivity and shear stress through the amount and distribution of leaf and stem biomass. The relationships among α, z_0, LAI, and H are plotted in Fig. 2, on the basis of the collected data in this study. Despite considerable scattering among them, it can be observed that all of these four parameters are interrelated. It means that, even though there is no direct physical relation between α and z_0, a functional relationship could be conceptually expressed by canopy structural parameters of LAI and H.

In order to confirm whether a negative linear relationship between α and z_0 is mainly caused by vegetation structure or not, we use the ratio of LAI to H (LAI/H) as the canopy structure parameter. In Fig. 3, it can be seen that the ratio (slope) of H to LAI is variable. For example, most leaves have the tendency to spread on the top of the canopy in order to better absorb light energy and form an optimal overlapped formation (Enquist et al. 1998). Hence, the exponent of the exponential curve between H and LAI in Fig. 3 reasonably represents the characteristics of the canopy structure.

Figure 4 shows the scatter plot between the ratio of log (z_0) to α and log-scaled LAI/H. Generally, when log(LAI/H) decreases, $\log(z_0)/\alpha$ increases because z_0 increases and α decreases. A relatively lower density of vegetation biomass represented by a low LAI/H value has a more exposed outer canopy surface; thus, α is low because of high rugosity and z_0 is large because of large frontal areas. The dashed fitted line in Fig. 4 is calculated on the basis of the fitted relationships for the above pattern (less than about 5 value of $\log(z_0)/\alpha$). That fitted correlation line shows that the relationship between α and $\log(z_0)$ (as shown in Fig. 1) can be dictated by the canopy structure complexity indicated by the ratio of LAI to H, which is governed by the allometric scaling law.

However, the point with the highest $\log(z_0)/\alpha$ value (marked by the arrow in Fig. 4) shows deviation from the fitted line. This point corresponds to the one at the upper-left corner of Fig. 1, which has the lowest α and highest z_0, and also has a relatively high LAI as compared to the fitted line given the same $\log(z_0)/\alpha$ value. For this point with dense greenness cover, LAI=8.4 and H=27.2, and although α has approached the minimum value (~0.05; see Fig. 1), z_0 can still increase because of increased shear drags, which explains why it falls far from the fitted line. Therefore, $\log(z_0)/\alpha$ will increase slightly at the low log (LAI/H) values at high LAI. On the other hand, a decrease in z_0 at extremely dense forest probably can be expected due to the flow skim over canopy tops without beating obstacles. In that case, a certain plot of high $\log(z_0)/\alpha$ value (greater than about 5) will be closer to the calculated line in Fig. 4.

Conclusions

The empirical α–z_0 relationship identified in this study needs to be examined whether the result remains valid when additional data from various vegetation types and environmental conditions are available. For instance, we

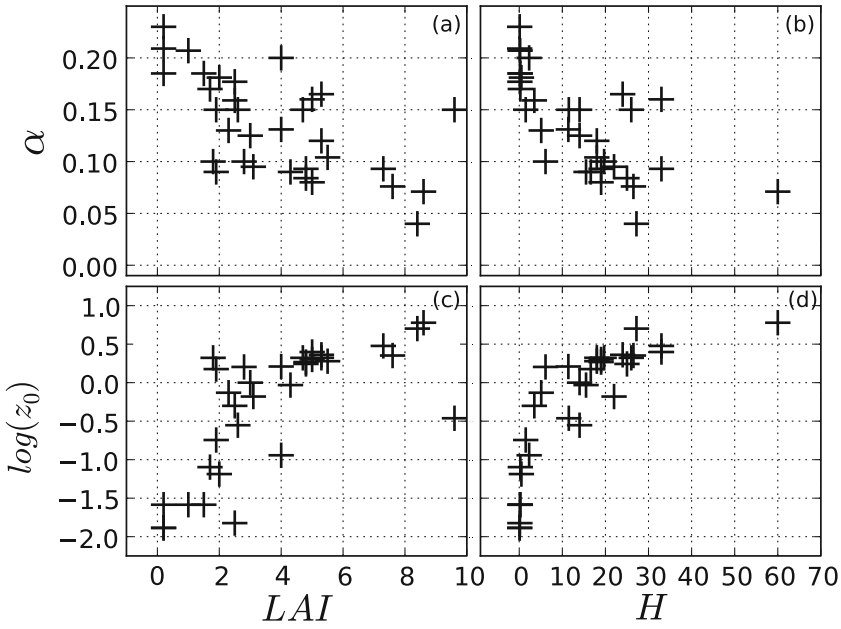

Fig. 2 Scatter plots between **a** *LAI* and α, **b** *H* and α, **c** *LAI* and log(z_0), **d** *H* and log(z_0). α albedo (dimensionless), z_0 roughness length (m), *H* canopy height (m),; *LAI* leaf area index (m^2 m^{-2}) based on data collected in this study

have only examined four broadly classified major vegetation types (forest, grassland, shrub, and crop); however, the case of tundra is not included in our analysis. Mosses and lichens in tundra have lower α than bare ground because of low reflectance of the chlorophyll contained in them. However, z_0 of tundra is likely to be similar to that of semi-desert because of the tiny size of tundra plants on the landscape scale (Oke 1987). In addition, the low land cover of tundra exposes the wet land surface area, which may also weaken the relationship between α and z_0.

Our result using limited measurement data may not be regarded as universally or absolutely characteristic when considering complex plant ecosystems. Hence, further work is warranted in identifying the causes of the scatters in the α–z_0 relationship. Thus, if a tighter relationship for various vegetation types, particularly in Figs. 1 and 4, is to be sought, then more field data under controlled environmental conditions are needed. However, our test of our hypothesis that there is a functional relationship between α and z_0 can nevertheless be extremely valuable in the understanding of the key land properties between the biosphere–atmosphere interactions. This work is divided into two main themes as described below.

First, α and z_0 are the main parameters to control the responses of vegetation and land cover changes in the climate model simulations. They are generally the default parameter pair. However, the existence of the α–z_0 relationship means that both are proportionally sensitive to each other, not the individual parameters themselves. Therefore, the identified relationship can serve as the basis for the development of more realistic optimized parameterizations in climate modeling studies. For example, the variation in the exchange of heat, moisture, and carbon due

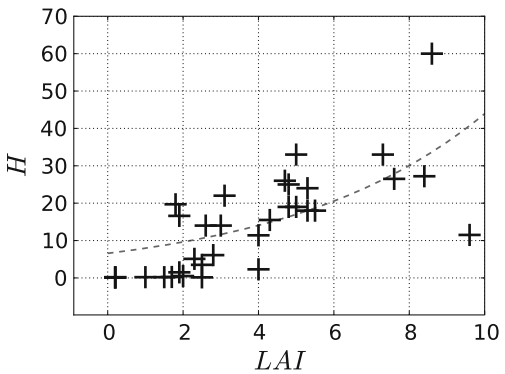

Fig. 3 Scatter plots between *LAI* and *H*. The *dashed line* is the correlation between *H* and *LAI*; H=6.57 exp(0.19 LAI) (R^2=0.67)

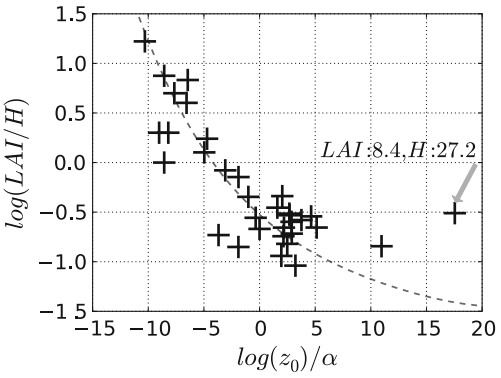

Fig. 4 Scatter plot between the ratio of the logarithm of z_0 to a log (z_0)/α and log-scaled ratio of *LAI* to *H*. *Dashed line* is calculated by fitted relationships with data of (log(z_0)/α < 5)

to vegetation structural changes can be traced continuously at each natural successive or anthropogenic deforestation stage.

Second, the potential of using space-based observations to derive surface α estimates has been recognized since the 1980s (Saunders 1990). The satellite-derived data are useful for estimating α on a large scale (Zhou et al. 2003). In contrast, satellite-based measurements of z_0 are far more difficult and less practical, primarily due to difficulties such as the necessity of field observations to validate the estimation and the assumption of geometrical canopies from the Poisson distribution (Schaudt and Dickinson 2000; Jasinski et al. 2005). The developed α–z_0 relationship of the basis on this study can thus be utilized to estimate large-scale distribution of z_0 from the satellite-based α imagery

Acknowledgements We would like to thank anonymous reviewers, whose comments were useful for revising this manuscript. This work was supported by JSPS KAKENHI, Grants-in-Aid for Scientific Research on Innovative Areas (22119009) and (S)(19106008), and Innovative program of climate change projection for the 21st Century from The Ministry of Education, Culture, Sports, Science and Technology (MEXT).

References

Baldocchi D, Falge E, Gu L, Olson R, Hollinger D, Running S, Anthoni P, Bernhofer C, Davis K, Evans R, Fuentes J, Goldstein A, Katul G, Law B, Lee X, Malhi Y, Meyers T, Munger W, Oechel W, Paw UKT, Pilegaard K, Schmid HP, Valentini R, Verma S, Vesala T, Wilson K, Wofsy S (2001) FLUXNET: a new tool to study the temporal and spatial variability of ecosystem-scale carbon dioxide, water vapor and energy flux densities. Bull Am Meteorol Soc 82:2415–2434

Berbigier P, Bonnefond J-M, Mellmann P (2001) CO_2 and water vapour fluxes for 2 years above Euroflux forest site. Agric For Meteorol 108:183–197

Beringer J, Chapin FS III, Thompson CC, McGuire AD (2005) Surface energy exchanges along a tundra-forest transition and feedbacks to climate. Agric For Meteorol 131:143–161

Betts AK, Desjardins RL, Worth D (2007) Impact of agriculture, forest and cloud feedback on the surface energy budget in BOREAS. Agric For Meteor 142:156–169

Betts RA, Cox PM, Lee SE, Woodward FI (1997) Contrasting physiological and structural vegetation feedbacks in climate change simulations. Nature 387:796–799

Bonan GB (2002) Ecological climatology. Cambridge University Press, New York

Brutsaert W (1982) Evaporation into the atmosphere; theory, history, and application. Kluwer, Dordrecht

Campbell GS (1973) An introduction to environmental biophysics. Springer, New York

Chen JM, Govind A, Sonnentag O, Zhang Y, Barr A, Amiro B (2006) Leaf area index measurements at Fluxnet-Canada forest sites. Agric For Meteorol 140:257–268

Choudhury BJ, Monteith JL (1988) A four-layer model for the heat budget of homogeneous land surfaces. Q J R Meteorol Soc 114:373–398

Cook BD, Davis KJ, Wang W, Desai A, Berger BW, Teclaw RM, Martin JG, Bolstad PV, Bakwin PS, Yi C, Heilman W (2004) Carbon exchange and venting anomalies in an upland deciduous forest in northern Wisconsin, USA. Agric For Meteorol 126:271–295

Coulter RL, Pekour MS, Cook DR, Klazura GE, Martin TJ, Lucas JD (2006) Surface energy and carbon dioxide fluxes above different vegetation types within ABLE. Agric For Meteorol 136:147–158

Dolman AJ, Moors EJ, Elbers JA (2002) The carbon uptake of a mid latitude pine forest growing on sandy soil. Agric For Meteorol 111:157–170

Eagleson PS (2002) Ecohydrology: Darwinian expression of vegetation form and function. Cambridge University Press, Cambridge

Enquist BJ, Brown JH, West GB (1998) Allometric scaling of plant energetic and population density. Nature 395:163–165

Garratt JR (1994) The Atmospheric Boundary Layer. Cambridge University Press, Cambridge

Green DG, Klomp N, Rimmington G, Sadedin S (2006) Complexity in landscape ecology. Springer, Netherlands

Grünwald T, Bernhofer C (2007) A decade of carbon, water and energy flux measurements of an old spruce forest at the Anchor Station Tharandt. Tellus Ser B 59:387–396

Gu L, Meyers T, Pallardy SG, Hanson PJ, Yang B, Heuer M, Hosman KP, Riggs JS, Sluss D, Wullschleger SD (2006) Direct and indirect effects of atmospheric conditions and soil moisture on surface energy partitioning revealed by a prolonged drought at a temperate forest site. J Geophys Res 111:D16102. doi:10.1029/2006JD007161

Hahmann AN, Dickinson RE (1997) RCCM2-BATS models over tropical South America: application to tropical deforestation. J Climate 10:1944–1964

Hattori S, Tamai K, Abe T (1993) Effects of soil moisture and vapor pressure deficit on evapotranspiration in a hinoki plantation. J Jpn For Soc 75:216–224 (in Japanese with English summary)

Henderson-Sellers A, Dickinson RE, Durbidge TB, Kennedy PJ, McGuffie K, Pitman AJ (1993) Tropical deforestation: modeling local- to regional-scale climate change. J Geophys Res 98:7289–7315

Hirose T (2005) Development of the Monsi-Saeki theory on canopy structure and function. Ann Bot 95:483–494

Hollinger DY, Ollinger SV, Richardson AD, Meyers TP, Dail DB, Martin ME, Scott NA, Arkebauer TJ, Baldocchi DD, Clark KL, Curtis PS, Davis KJ, Desai AR, Dragoni D, Goulden ML, Gu L, Katul GG, Pallardy SG, Paw UKT, Schmid HP, Stoy PC, Suyker AE, Verma SB (2010) Albedo estimates for land surface models and support for a new paradigm based on foliage nitrogen concentration. Glob Change Biol 16:696–710

Jarvis PG, James GB, Landsberg JJ (1976) Coniferous forest. In: Monteith JL (ed) Vegetation and the atmosphere, vol 2. Academic, London, pp 171–240

Jasinski MF, Borak J, Crago R (2005) Bulk surface momentum parameters for satellite-derived vegetation fields. Agric For Meteorol 133:55–68

Kanae S, Oki T, Musiake K (2001) Impact of deforestation on regional precipitation over the Indochina peninsula. J Hydrometeorol 2:51–70

Klaassen W, van Breugel PB, Moors EJ, Nieveen JP (2002) Increased heat fluxes near a forest edge. Theor Appl Climatol 72:231–243

Knohl A, Schulze E-D, Kolle O, Buchmann N (2003) Large carbon uptake by an unmanaged 250-years-old deciduous forest in Central Germany. Agric For Meteorol 118:151–167

Laurila T, Soegaard H, Lloyd CR, Aurela M, Tuovinen J-P, Nordstroem C (2001) Seasonal variations of net CO_2 exchange in European Arctic ecosystems. Theor Appl Climatol 70:183–201

Lean J, Warrilow DA (1989) Simulation of the regional climatic impact of Amazon deforestation. Nature 342:411–413

Lettau H (1969) Note on aerodynamic roughness-parameter estimation on the basis of roughness-element description. Appl Meteorol 8:828–832

Leuning R, Raupach MR, Coppin PA, Cleugh HA, Isaac P, Denmead OT, Dunin FX, Zegelin S, Hacker J (2004) Spatial and temporal variations in fluxes of energy, water vapour and carbon dioxide during OASIS 1994 and 1995. Boundary-Layer Meteorol 110:3–38

Li SG, Harazono Y, Oikawa T, Zhao HL, He ZY, Chang XL (2000) Grassland desertification by grazing and the resulting micrometeorological changes in Inner Mongolia. Agric For Meteor 102:125–137

Mahrt L, Ek M (1993) Spatial variability of turbulent fluxes and roughness lengths in HAPEX-MOBILHY. Boundary-Layer Meteorol 65:381–400

Martano P (2000) Estimation of surface roughness length and displacement height from single-level sonic anemometer data. J Appl Meteorol 39:708–715

Mihailović DT, Kallos G (1997) Sensitivity study of a coupled soil-vegetation boundary-layer scheme for use in atmospheric modeling. Boundary-Layer Meteorol 82:283–315

Mölder M, Lindroth A (1999) Thermal roughness length of a boreal forest. Agric For Meteorol 98–99:659–670

Monteith JL, Unsworth MH (2008) Principles of environmental physics, 3rd edn. Academic, San Diego

Nakai T, Sumida A, Daikoku K, Matsumoto K, van der Molen MK, Kodama Y, Kononov AV, Maximov TC, Dolman AJ, Yabuki H, Hara T, Ohta T (2008) Parameterization of aerodynamic roughness over boreal, cool- and warm-temperate forests. Agric For Meteor 148:1916–1925

Ogunjemiyo S, Parker G, Roberts D (2005) Reflections in bumpy terrain: implications of canopy surface variations for the radiation balance of vegetation. IEEE Geosci Remote Sens Lett 1:90–93

Ohtani Y, Mizoguchi Y, Watanabe T, Yasuda Y, Okano M (2001) Seasonal change of CO_2 flux above an evergreen needle leaf forest in temperate region, Fujiyoshida, Japan. Proc. international workshop for advanced flux network and flux evaluation. (eds. Fujinuma Y, Takada M, Tashiro K, Nagahama T, Abe M, Hagiwara T, Zeng J) Center for Global Environmental Research, Tukuba, pp 129–132

Oke TR (1987) Boundary layer climates, 2nd edn. Halsted, London

Ollinger SV, Richardson AD, Martin ME, Hollinger DY, Frolking SE, Reich PB, Plourde LC, Katul GG, Munger JW, Oren R, Smith M-L, Paw UKT, Bolstad PV, Cook BD, Day MC, Martin TA, Monson RK, Schmid HP (2008) Canopy nitrogen, carbon assimilation, and albedo in temperature and boreal forests: Functional relations and potential climate feedbacks. Proc Natl Acad Sci USA 105:19336–19341

Parker GG (1995) Structure and microclimate of forest canopies. In: Lowman MD, Nadkarni NM (eds) Forest canopies. .Academic, San Diego, pp 73–106

Parker GG, Russ ME (2004) The canopy surface and stand development: assessing forest canopy structure and complexity with near-surface altimetry. Agric For Meteor 189:307–315

Price CA, Enquist BJ, Savage VM (2007) A general model for allometric covariation in botanical form and function. Proc Natl Acad Sci USA 104:13204–13209

Raupach MR (1994) Simplified expressions for vegetation roughness length and zero-displacement as a function of canopy height and area index. Boundary-Layer Meteorol 71:211–216

Saunders R (1990) The determination of broad band surface albedo from AVHRR visible and near-infrared radiance. Int J Remote Sens 11:49–67

Schaudt KJ, Dickinson RE (2000) An approach to deriving roughness length and zero-plane displacement height from satellite data, prototyped with BOREAS data. Agric For Meteorol 104:143–155

Schmid HP, Grimmond SB, Cropley F, Offerle B, Su H-B (2000) Measurements of CO_2 and energy fluxes over a mixed hardwood forest in the mid-western United States. Agric For Meteorol 103:357–374

Sellers PJ (1985) Canopy reflectance, photosynthesis and transpiration. Int J Remote Sens 6:1335–1372

Sellers PJ, Dickinson RE, Randall DA, Betts AK, Hall FG, Berry JA, Collatz GJ, Denning AS, Mooney HA, Nobre CA, Sato N, Field CB, Henderson-Sellers A (1997) Modeling the exchanges of energy, water, and carbon between continents and the atmosphere. Science 275:502–509

Shuttleworth WJ, Leuning R, Black TA, Grace J, Jarvis PG, Roberts J, Jones HG (1989) Micrometeorology of temperate and tropical forest. Philos Trans R Soc Lond B 324:299–334

Stanhill G (1970) Some results of helicopter measurements of albedo. Sol Energy 13:59–66

Suni T, Rinne J, Reissell A, Altimir N, Keronen P, Rannik U, Maso MD, Kulmala M, Vesala T (2003) Long-term measurements of surface fluxes above a Scots pine forest in Hyytiala, southern Finland, 1996–2001. Boreal Environ Res 8:287–301

Thomas C, Foken T (2007) Organized motion in a tall spruce canopy: temporal scales, structure spacing and terrain effects. Boundary-Layer Meteorol 122:123–147

Thomas SC, Winner WE (2000) Leaf area index of an old-growth Douglas-fir forest estimated from direct structural measurements in the canopy. Can J For Res 30:1922–1930

Thompson C, Beringer J, Chapin FS III, McGuire AD (2004) Structural complexity and land-surface energy exchange along a gradient from arctic tundra to boreal forest. J Veg Sci 15:397–406

Turnipseed AA, Anderson DE, Blanken PD, Baugh WM, Monson RK (2003) Airflows and turbulent flux measurements in mountainous terrain; Part.1 Canopy and local effects. Agric For Meteorol 119:1–21

Wang J, Bastiaanssen WGM, Ma Y, Pelgrum H (1998) Aggregation of land surface parameters in the oasis-desert systems of north-west China. Hydrol Process 12:2133–2147

Wooding RA, Bradley EF, Marshall JK (1973) Drag due to regular arrays of roughness elements of varying geometry. Boundary-Layer Meteorol 5:285–308

Zhou L, Dickinson RE, Tian Y, Zeng X, Dai Y, Yang Z-L, Schaaf CB, Gao F, Jin Y, Strahler A (2003) Comparison of seasonal and spatial variations of albedos from Moderate-Resolution Imaging Spectroradiometer (MODIS) and Common Land Model. J Geophys Res 108:4488. doi:10.1029/2002JD003326